XL CILAMCE
IBERO-LATIN AMERICAN CONGRESS ON COMPUTATIONAL METHODS IN ENGINEERING
NOVEMBER 11-14, 2019
Praiamar Natal Hotel & Convention
Natal, RN-BRAZIL

MECHANICAL PERFORMANCE ANALYSIS OF PLATES FROM APPROXIMATED METHOD

Edmilson Lira Madureira
E-mail: edmadurei@yahoo.com.br
Gabriel de Bessa Spinola
Email: gabrielbessasp@gmail.com
Arthur Leandro de Azevedo Silva
E-mail: arthur_leandro33@hotmail.com
Eduardo Morais de Medeiros
E-mail: mm.edu@hotmail.com
Departamento de Engenharia Civil – Universidade Federal do Rio Grande do Norte
Av. Sen. Salgado Filho S/N - CEP 59072 –970 – Lagoa Nova, Natal, Rio Grande do Norte, Brasil

Abstract. Due to the lack of consensus among the several models applied to its internal forces assessment, the design of slabs represents a task of reasonable complexity. The availability of high-performance software allows its mechanical performance simulation from the continuous plate concept. Despite its great acceptability the results obtained from such procedure are far from the reality since the knowledge domain of the mechanical behavior of concrete yet did not reached fullness. The validation of software's can be performed by using simplified procedures adopting in hand calculation or small algorithms. Such kinds of approaches are useful, including, as design resources for more modest constructive units, namely, residential buildings or small commercial and industrial structures. The Thin Plates Theory is applied to solid bodies composed by linear, elastic and homogeneous material, whose thickness is inferior to its remaining dimensions. Some solutions of the Differential Equation, derived from the referring Model, were proposed by Navier and by Levi. The aim of this work is the analysis of mechanical performance of reinforced concrete slabs, layered upon a group of high stiffness beams, from the Thin Plates Theory considering the solutions proposed by Navier and by Levi. The obtained results have revealed that, even for that cases involving symmetrical loading and edge conditions, the maximum bend moment in the "y" direction occur at a point deviated from the center of the plate, and its magnitude is greater than that one recorded at the plate center.

Keywords: Reinforced concrete, Plates, Mechanical performance, Analysis.

1 Introduction

The Grid Method, The Marcus Method and the Thin Plate Theory represent models suitable to perform the analysis of displacements and internal Forces. Due to the lack of consensus of these models that has endured until nowadays, the reinforced concrete slabs design involves approach tasks of reasonable complexity.

The availability of high-performance computational codes allows the slabs mechanical performance simulation from plate elements and the assessment of the mechanical performance parameters from the consideration of their continuity. Nevertheless, the resolution carried out in this way is far from culminating into irrefutable results due to the fact that the knowledge domain of the concrete behavioral response is yet to achieve fullness.

The validating operation of the obtained results referring to slabs analysis from automatic codes can be performed from the adoption of suitable simplified procedures for in hand calculation or small algorithms implementation.

Such kind of simplified approaches are useful, including, as design resources of more modest constructive units projects, namely, buildings to support residences or commercial and industrial activities of low magnitude.

The Kirchhoff's model, which culminates in the Thin Plates Theory, is applied to those cases involving structural solids composed by linear elastic homogeneous and isotropic material, of thickness that is very inferior to its dimensions in plant, for which, including, the Bernoulli hypothesis is valid.

A partial differential equation, namely, the Differential Equation of the Plates, is associated to the Kirchhoff's Model, whose solution, for some special cases, was proposed by Navier and by Levi.

The aim of this work is the analysis of the mechanical performance of reinforced concrete slabs from the Thin Plates Theory considering the solutions proposed by Navier and by Levi.

Such analysis proceeding is applied to models consisting by laminar structures layered on a group of high stiffness beams that can be regarded as no displaceable supports.

The structural members defined according this mode are diversified into a set of cases distinguished from each to another by geometric characteristics, taking into account, specially, the establishment of, at least, three different ratios between the span lengths, in the two principal coordinate directions.

2 Modelling

According to the Classical Theory of the Elasticity, the bending stiffness of plates is written in the form:

$$D = \frac{Eh^3}{12(1-\nu^2)} \quad (1)$$

for which the E and υ parameters represent, respectively, the modulus of elasticity and the Poisson's ratio of the plate constituent material, while the h parameter is the plate thickness.

For the plate shown in Fig. 1.a, its deformed shape, Fig. 1.b, is described by the Lagrange Differential Equation, which stems from the Kirchhoff's Thin Plates theory, and is of the form presented by Woinowsky-Krieger and Timoshenko [1], and by Szilard [2], expressed by:

$$\frac{\partial^4 \omega}{\partial x^4} + 2\frac{\partial^4 \omega}{\partial x^2 \partial y^2} + \frac{\partial^4 \omega}{\partial y^4} = \frac{p_z(x,y)}{D} \quad (2)$$

since $p_z(x,y)$ is the load distribution function over the surface wide area of the plate.

According Szilard [2], the solution proposed by Navier for such differential equation, applied, solely, to plates that are simply supported along its all four edges, Figure 2.a, is expressed by a double trigonometric series, as presented in Eq.(3).

$$w(x,y) = \sum_{m=1}^{\infty}\sum_{n=1}^{\infty} W_{mn} sin\left(\frac{m\pi x}{L_x}\right) sin\left(\frac{n\pi y}{L_y}\right) \tag{3}$$

such that, the "L_x" and "L_y" parameters, are the span lengths over the "x" and "y" coordinate directions, respectively. Equation (3) is valid as long as it is possible to approximate the transverse load for the trigonometric and also double series:

$$p_z(x,y) = \sum_{m=1}^{\infty}\sum_{n=1}^{\infty} P_{mn} sin\left(\frac{m\pi x}{L_x}\right) sin\left(\frac{n\pi y}{L_y}\right) \tag{4}$$

According the Fourier's Middle Period Series concept, the "P_{mn}" parameter is the, so called, Fourier's Coefficient and it is obtained from the Euler's form:

$$P_{mn} = \frac{4}{L_x L_y}\int_0^{L_y}\int_0^{L_x} p_z(x,y)\ sin\left(\frac{m\pi x}{L_x}\right) sin\left(\frac{n\pi y}{L_y}\right) dxdy \tag{5}$$

Once replacing Eq. (3) and Eq. (4) into Eq. (2) and promoting relevant algebraic transformations, it may result:

$$P_{mn} = \left[\left(\frac{m}{L_x}\right)^2 + \left(\frac{n}{L_y}\right)^2\right]^2 \pi^4 D W_{mn} \tag{6}$$

and,

$$W_{mn} = \frac{P_{mn}}{\left[\left(\frac{m}{L_x}\right)^2 + \left(\frac{n}{L_y}\right)^2\right]^2 \pi^4 D} \tag{7}$$

If Eq (7) is considered in Eq. (3) this later equation assumes the form of the relationship:

$$\mathrm{w(x,y)} = \sum_{\mathrm{m=1}}^{\infty}\sum_{\mathrm{n=1}}^{\infty} \frac{\mathrm{P_{mn}}}{\left[\left(\frac{\mathrm{m}}{\mathrm{L_x}}\right)^2 + \left(\frac{\mathrm{n}}{\mathrm{L_y}}\right)^2\right]^2 \pi^4 \mathrm{D}} \sin\left(\frac{\mathrm{m\pi x}}{\mathrm{L_x}}\right) \sin\left(\frac{\mathrm{n\pi y}}{\mathrm{L_y}}\right) \tag{8}$$

If the load is uniformly distributed and p is its magnitude, then:

$$P_{mn} = \frac{16p}{\pi^2 mn}\ \ and\ W_{mn} = \frac{16p}{\left[\left(\frac{m}{L_x}\right)^2 + \left(\frac{n}{L_y}\right)^2\right]^2 \pi^6 mnD}, m,n = 1,3,5 \tag{9}$$

The bend moments, Fig. 1.c, are expressed, according the Kirchhoff's Theory from de mathematical sentences:

$$M_x = -D\left(\frac{\partial^2\omega}{\partial x^2} + \nu\frac{\partial^2\omega}{\partial y^2}\right)\ e\ M_y = -D\left(\nu\frac{\partial^2\omega}{\partial x^2} + \frac{\partial^2\omega}{\partial y^2}\right) \tag{10}$$

while the twisting moments are described according the equation:

$$M_{xy} = -(1-\nu)D\frac{\partial^2\omega}{\partial x \partial y} \tag{11}$$

If Eq. 8 is replaced into Eq. 10 and Eq. 11, it may be obtained:

$$M_x = \pi^2 D\sum_{m=1}^{\infty}\sum_{n=1}^{\infty}\left[\left(\frac{m}{L_x}\right)^2 + \nu\left(\frac{n}{L_y}\right)^2\right] W_{mn} sin\left(\frac{m\pi x}{L_x}\right) sin\left(\frac{n\pi y}{L_y}\right) \tag{12}$$

$$M_y = \pi^2 D \sum_{m=1}^{\infty}\sum_{n=1}^{\infty}\left[\nu\left(\frac{m}{L_x}\right)^2 + \left(\frac{n}{L_y}\right)^2\right] W_{mn} sin\left(\frac{m\pi x}{L_x}\right) sin\left(\frac{n\pi y}{L_y}\right) \quad (13)$$

and:

$$M_{xy} = M_{yx} = -(1-\nu)\pi^2 D \sum_{m=1}^{\infty}\sum_{n=1}^{\infty}\frac{mn}{L_x L_y} W_{mn} cos\left(\frac{m\pi x}{L_x}\right) cos\left(\frac{n\pi y}{L_y}\right) \quad (14)$$

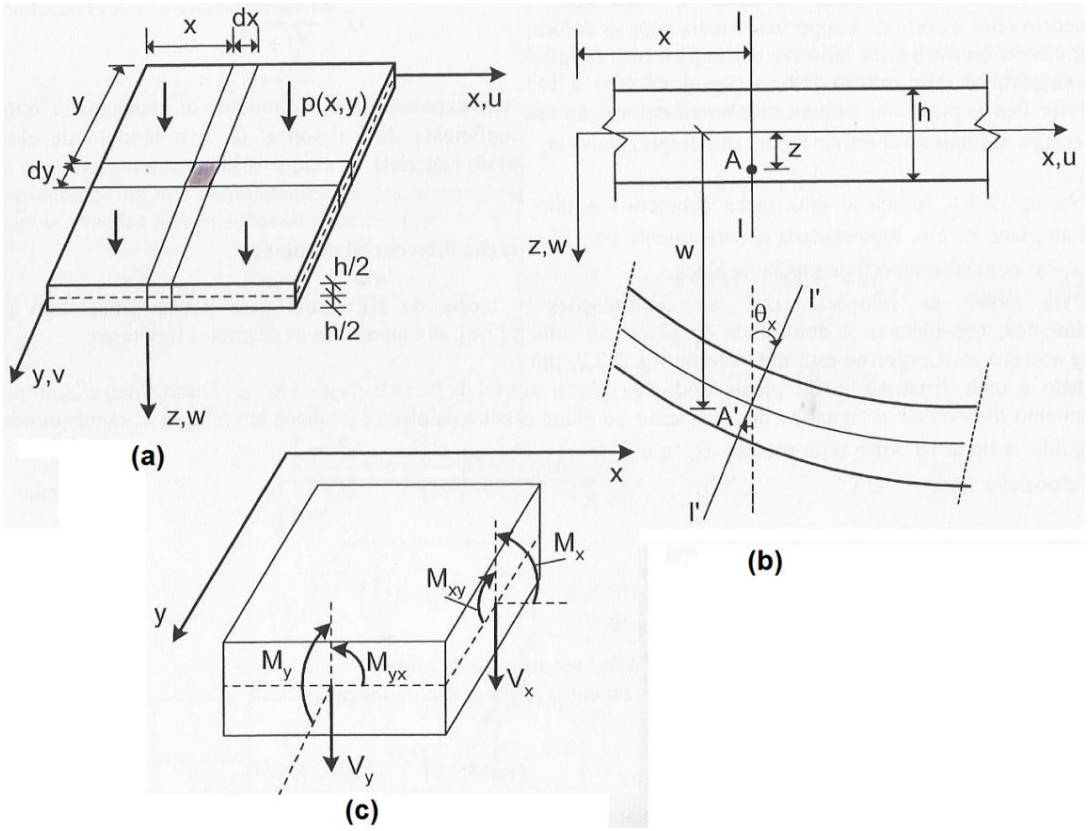

Figure 1. a) Slab; b) Deformed shape; c) Internal forces

As it was presented by Szilard [2], the solution of the Differential Equation of the Plates proposed by Levi, applied to slabs presenting the boundary conditions indicating in Fig. 2.a is of the form:

$$\omega(x,y) = \sum_{m=1}^{\infty}\left[A_m cosh\left(\frac{m\pi x}{L_y}\right) + B_m \frac{m\pi x}{L_y} sinh\left(\frac{m\pi x}{L_y}\right) + W_m\right] sin\left(\frac{m\pi y}{L_y}\right) \quad (15)$$

For which:

$$W_m = \frac{4L_y^4}{(m\pi)^5}\frac{p}{D}; \alpha_m = \frac{m\pi L_x}{2L_y};\ B_m = \frac{W_m}{2\cos h(\alpha_m)}\ and\ A_m = -\frac{B_m \alpha_m senh(\alpha_m) + W_m}{\cos h(\alpha_m)}$$

Replacing Eq. (15) into Eq. (10) and Eq. (11), it may result:

$$M_x = D\frac{\pi^2}{{L_x}^2}\sum_{m=1}^{\infty} m^2 \left\{[(1-\nu)A_m - 2\nu B_m]cosh\left(\frac{m\pi x}{L_y}\right) + (1-\nu)B_m \frac{m\pi x}{L_y} senh\left(\frac{m\pi x}{L_y}\right) + W_m\right\} sen\left(\frac{m\pi y}{L_y}\right) \quad (16)$$

$$M_y = D\frac{\pi^2}{{L_x}^2}\sum_{m=1}^{\infty} m^2\left\{[(\nu-1)A_m - 2B_m]cosh\left(\frac{m\pi x}{L_y}\right) + (\nu-1)B_m\frac{m\pi x}{L_y}senh\left(\frac{m\pi x}{L_y}\right) + \nu W_m\right\}sen\left(\frac{m\pi y}{L_y}\right) \quad (17)$$

and:

$$M_{xy} = -(1-\nu)\frac{\pi^2 D}{{L_x}^2}\sum_{m=1}^{\infty} m^2\left[(A_m + B_m)senh\left(\frac{m\pi x}{L_y}\right) + B_m\frac{m\pi x}{L_y}cosh\left(\frac{m\pi x}{L_y}\right)\right] \cdot cos\left(\frac{m\pi y}{L_y}\right) \quad (18)$$

As it is described by Szilard [2], Eq. 15, 16, 17 and 18 may be applied, too, for the structural analysis of slabs presenting the boundary conditions indicating in Fig. 2.b, since it is considered that:

$$B_m = \frac{W_m senh(\alpha_m)}{\alpha_m + senh(\alpha_m)\cos h(\alpha_m)} \quad (19)$$

For slabs presenting the boundary conditions illustrated on Fig. 2.c, the solution of the Differential Equation of the Plates proposed by Levi is of the form:

$$\omega(x,y) = \sum_{m=1}^{\infty}\left\{\left[A_m + D_m\frac{m\pi x}{L_y}\right]cosh\left(\frac{m\pi x}{L_y}\right) + \left[B_m\frac{m\pi x}{L_y} + C_m\right]senh\left(\frac{m\pi x}{L_y}\right) + W_m\right\}sen\left(\frac{m\pi y}{L_y}\right) \quad (20)$$

since that, the "A_m", "B_m", "C_m" and "D_m" parameters are obtained from the set of equations 21, 22, 23 and 24, solution.

$$cosh(\alpha_m)A_m + \alpha_m senh(\alpha_m)B_m - senh(\alpha_m)C_m - \alpha_m cosh(\alpha_m)D_m = -W_m \quad (21)$$

$$cosh(\alpha_m)A_m + \alpha_m senh(\alpha_m)B_m + senh(\alpha_m)C_m + \alpha_m cosh(\alpha_m)D_m = -W_m \quad (22)$$

$$senh(\alpha_m)A_m + [senh(\alpha_m) + \alpha_m cosh(\alpha_m)]B_m - cosh(\alpha_m)C_m - [cosh(\alpha_m) + \alpha_m senh(\alpha_m)]D_m = 0 \quad (23)$$

$$cosh(\alpha_m)A_m + [2cosh(\alpha_m) + \alpha_m senh(\alpha_m)]B_m + senh(\alpha_m)C_m + [2senh(\alpha_m) + \alpha_m cosh(\alpha_m)]D_m = 0 \quad (24)$$

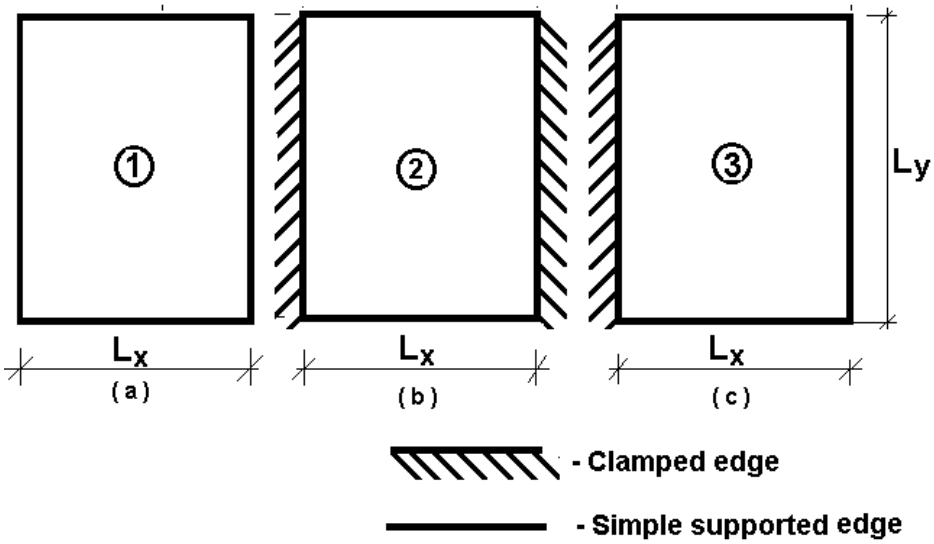

Figure 2. Plates boundary conditions

The bending and the twisting moments may be obtained by Eq. 10 and Eq. 11, respectively.

The tables prepared by Barés, presented by Araújo [3], exhibit dimensionless parameters in terms of displacement and internal forces and are determined from the theory of plates, which should be employed for the final displacements and internal forces calculations.

With the view to carry out the plate structural analysis on the base of the Finite Element Technique Eq. 10 and Eq. 11 may be written in the matrix form:

$$\{M\} = -|D_k|\{k\} \tag{25}$$

The moments matrix is expressed by:

$$\{\mathrm{M}\} = \begin{bmatrix}\mathrm{M_x} & \mathrm{M_y} & \mathrm{M_{xy}}\end{bmatrix}^{\mathrm{T}} \tag{26}$$

The stiffness is described in terms of the matrix:

$$[\mathrm{D_k}] = \mathrm{D}\begin{bmatrix}1 & \nu & 0 \\ \nu & 1 & 0 \\ 0 & 0 & \dfrac{1-\nu}{2}\end{bmatrix} \tag{27}$$

The bending curvature vector is given by:

$$\{\boldsymbol{k}\} = \begin{bmatrix}\dfrac{\partial^2 w}{\partial x^2} & \dfrac{\partial^2 w}{\partial y^2} & 2\dfrac{\partial^2 w}{\partial x \partial y}\end{bmatrix}^{\boldsymbol{T}} \tag{28}$$

Once the Kirchhoff's Theory is valid, solely, for that cases from which the strains due to the shear stresses are negligible, the mechanical deformation energy may be widely characterized in terms of the xy on plan strains "ε_x", "ε_y" e "γ_{xy}", and these strains may be written as a function of the transverse displacement w(x,y). The Kirchhoff's plate element may be formulated from the energy deformation presented by Cook et al [4], as the equation:

$$U = \int_V \frac{1}{2}\{k\}^T[D_k]\{k\}dA \tag{29}$$

For the four nodded element type, Fig. 3, it must be considered three degrees of freedom for each nodal point, namely, the transverse translation "w_i" and the rotations around the coordinate axis "$w_{,xi}$" and "$w_{,yi}$". On a mathematical meaning, the terms "$w_{,xi}$" and "$w_{,yi}$" represent the derivative of the "w_i" function relating to the "x" and the "y" variables, respectively. The shape functions, corresponding to "n" nodal points elements, may be represented from the vector:

$$\{N\} = [N_1 \;\; N_2 \;\; \ldots N_{3n}] \tag{30}$$

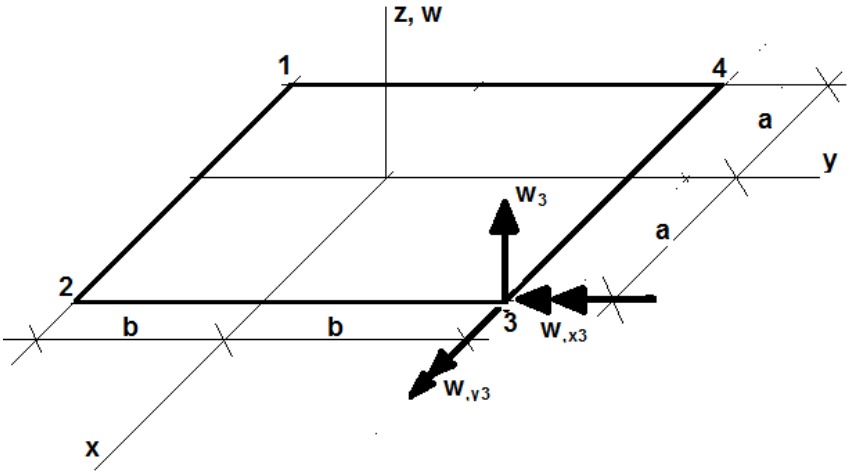

Figure 3. Four nodded Kirchhoff's Plate Element

If the nodal displacement vector referring to the plate element is as presented in Eq (31),

$$\{d\} = \left[w_1 \;\; w_{,x1} \;\; w_{,y1} \; . \; . \; . \; w_n \;\; w_{,xn} \;\; w_{,yn}\right]^T \tag{31}$$

the translational displacement normal to the middle plan of the plate, for any point placed in such a plan, will be expressed by:

$$w = [N]\{d\} \tag{32}$$

While, for the curvature vector results the relationship:

$$\{k\} = [B]\{d\} \tag{33}$$

The geometric matrix [B] in Eq. 33 presents 3x3n size, such that, the vector {k} will be 3 length and the vector {M} will be 3n length.

In the other hand, in the Grid Method formulation, the plates are discretized from finite unitary width tracks in both directions "x" and "y", and any interaction between two adjacent tracks is disregarded, highlighting the mechanical performance of two tracks each of them distributed along one of the coordinate direction and intersecting themselves at the center of the referring structural member.

The tracks so defined are treated as beams whose height is equal to the slab thickness and the continuity of the set of tracks is established, merely, from the condition that the vertical displacements at the center of their spans are equals to both beams that represent the perpendicular tracks intersecting at the referring point. The Mechanics of Solid Materials postulates are applied to derive the equations that must be used to determinate the displacements and internal forces. The twisting stiffness may be considered, in an approximate mode, from which the positive calculated moment magnitudes are reduced by the adoption of the coefficients proposed by Marcus, presented in Araújo [3].

3 Computational Support

In order to fulfill the objective proposed in this work, computational software was developed in automatic language C++**,** drafted upon the formulation affects to the grid method and those one referring to the solutions that were proposed by Navier and by Lévi. A computational image generator, elaborated in Delph, called PROJECT 2, Madureira and Silva [5], including, was used.

4 Computational Program Validation

The C++ computational program, characterized on the number 3 section of this paper, will be validated, naturally, in the course of this text development since the relevant subject of this work is a comparative structural analysis, based on several approximated models.

5 Analyzed Specimens

The analyzed specimens are laminar structural members cast by C 30 concrete, whose relevant physical parameters, namely, the Young's modulus and the Poisson's ratio, were, properly, evaluated in accordance to the NBR 6118/2014, Design of Structural Concrete – Procedure [6].

The analysis subject of this work will be performed upon slabs whose span length in the "x" coordinate direction is fixed as "L_x = 4,00 m", considering a set of cases differentiated among themselves by the boundary conditions illustrated in Fig. 2 and by their span lengths in the "y" coordinate direction, "L_y".

The analyzed specimens are submitted to uniformly distributed load normal to its middle plan.

The works reported in this paper were carried out from the consideration of two distinct stages of analysis. At the first one, 11(eleven) different span lengths in the "y" coordinate direction are considered, in order to establish the different and gradual values for the ratio "λ = Ly/Lx", namely: 1.0; 1.1; 1.2; 1.3; 1.4; 1.5; 1.6; 1.7; 1.8; 1.9 and 2.0. It was determined, therefore, the dimensionless parameters values for the bending moments over both coordinate directions and for the transverse

displacement, to allow the trend analysis. At the second stage of analysis it was performed the works on slabs presenting, alternatively, three values for the span length in the "y" coordinate direction, namely: "L_y = 4.00 m"; "L_y = 5.00 m"; and, "L_y = 6.00 m", and the relevant results comparison were established, and then the displacements and the moments variation fields along the whole area of the slabs were drafted.

6 Results

From the obtained results referring to the first stage of analysis, the folders of Fig. 4, 5, 6 and 7 were drafted, and, from such figures it may be noted close agreement, for the number one case, between the Lévi solution and the Navier double trigonometric series. In addition, it may be observed that the dimensionless parameters extracted from the Barés tables, agree in a fine approach with its corresponding results obtained by the Lévi solution.

According to the curves of Fig. 4 and the Table 1, the transverse displacement magnitude on the slab center, obtained from the Thin Plates Theory, proved to be smaller than those ones determined from the Grids Method as already reported by Silva e Cashell [7] and by Madureira et al [8].

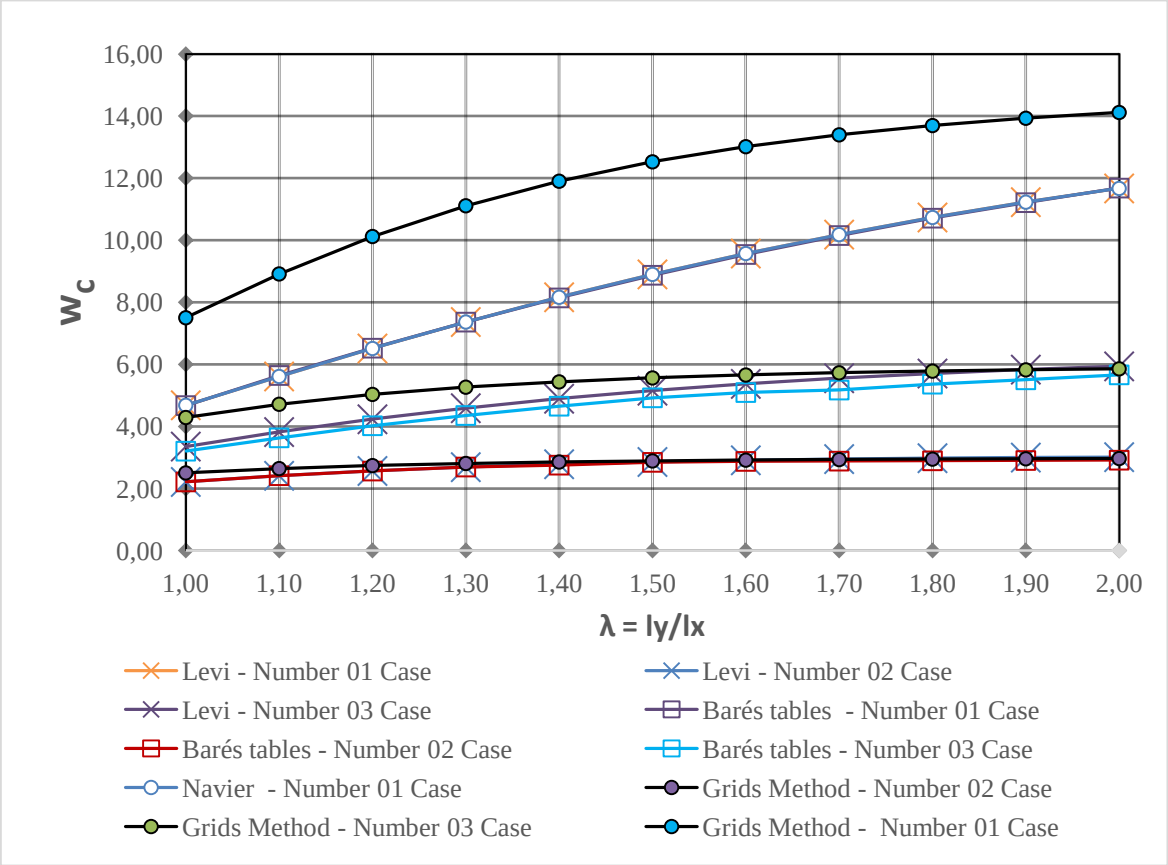

Figure 4. Transverse displacement dimensionless parameters

On the other hand, the bending moments at the center of slabs, over both coordinate directions, calculated from the Grid-Marcus Method, have presented smaller magnitudes than those ones referred in the upper paragraph, Fig. 5 and 6, while the results obtained from Grids Method present the highest values, Tables 2 and 3.

The differences among the displacement magnitudes reported above are as smaller as greater the ratio between the span lengths along the two coordinate directions, because, for the case number one, it was reduced from 37%, for λ = 1.0, to 17% for λ = 2.0, Table 1.

The differences involving the magnitudes of the positive bending moments in the "x" direction showed similar trend, ranging from 17% to 5%, if the results from the Theory of Plates and those ones

from Grid-Marcus Method are compared, and, ranging from 29% to 15%, if the results from the Theory of Plates and that ones from Grid Method are compared, Table 2.

The differences referring to the positive bending moments over the "y" coordinate direction, seem have presented the same trendy reported above in this paragraph, if the results from the Theory of Plates and that ones from the Grid Method are compared, decreasing from 29% to 15%. However, it may be observed that, at first, it occurs reduction in such difference if the ratio between the span lengths increases from $\lambda = 1.0$ up to $\lambda = 1.6$ and, after that, the difference tends to increase. On the other hand, if the results from the Theory of Plates and that ones from Grid/Marcus Method are compared, that difference presented diverse behavior, therefore, they increased from 24% up to 36%, since the "λ" values ranged from 1.0 up to 2.0, Table 3.

Table 1. Displacements dimensionless parameters

	Displacements – w_c					
	Number 01 Case		Number 02 Case		Number 03 Case	
λ	P	G	P	G	P	G
1.00	4.68	7.50	2.21	2.50	3.35	4.29
1.10	5.61	8.91	2.41	2.64	3.82	4.71
1.20	6.51	10.12	2.56	2.74	4.23	5.03
1.30	7.36	11.11	2.69	2.80	4.59	5.26
1.40	8.16	11.90	2.78	2.85	4.89	5.43
1.50	8.90	12.53	2.85	2.89	5.15	5.56
1.60	9.57	13.01	2.91	2.91	5.37	5.65
1.70	10.18	13.40	2.95	2.93	5.55	5.73
1.80	10.73	13.70	2.97	2.94	5.70	5.78
1.90	11.23	13.93	2.99	2.95	5.83	5.82
2.00	11.67	14.12	3.01	2.96	5.93	5.85
P – Plates Theory Data; G – Grid Method Data						

Table 2. Positive bending moment in “x” coordinate direction dimensionless parameters

	Bending Moment - M_x								
	Number 01 Case			Number 02 Case			Number 03 Case		
λ	P	G	GM	P	G	GM	P	G	GM
1.00	4.42	6.25	3.65	3.17	3.47	2.67	3.90	5.02	3.34
1.10	5.19	7.43	4.39	3.43	3.67	2.93	4.40	5.52	3.84
1.20	5.93	8.43	5.14	3.63	3.80	3.13	4.83	5.90	4.29
1.30	6.62	9.26	5.88	3.79	3.89	3.30	5.20	6.17	4.67
1.40	7.26	9.92	6.57	3.91	3.96	3.43	5.52	6.37	4.99
1.50	7.84	10.44	7.21	4.00	4.01	3.53	5.79	6.52	5.26
1.60	8.37	10.85	7.78	4.07	4.04	3.62	6.02	6.63	5.48
1.70	8.85	11.16	8.29	4.12	4.07	3.69	6.21	6.71	5.67
1.80	9.28	11.41	8.73	4.15	4.09	3.74	6.37	6.77	5.83
1.90	9.66	11.61	9.12	4.17	4.10	3.79	6.50	6.82	5.96
2.00	10.00	11.76	9.46	4.19	4.12	3.83	6.61	6.86	6.08
P – Plates Theory Data; G – Grid Method Data; Grid-Marcus Procedure Data									

For the cases 02 and 03 the behavioral trend was the same of that one related above in this text and was differentiated from the former, solely by the recorded values, Tables 1, 2 and 3. Nevertheless, it is worthwhile to highlight that the differences among the obtained values from Marcus-Grid Method and those ones calculated from the Theory of Plates, have resulted, significantly, smaller, and such differences was as smaller as greater was the slab bending stiffness as it may be seen in Figures 4, 5 and 6, and, in Tables 1, 2 and 3.

The acquired results reveal a satisfactory agreement among all the adopted data sources for the magnitude of the negative bending moments “M_{xe}”, as it may be note in Fig. 7.

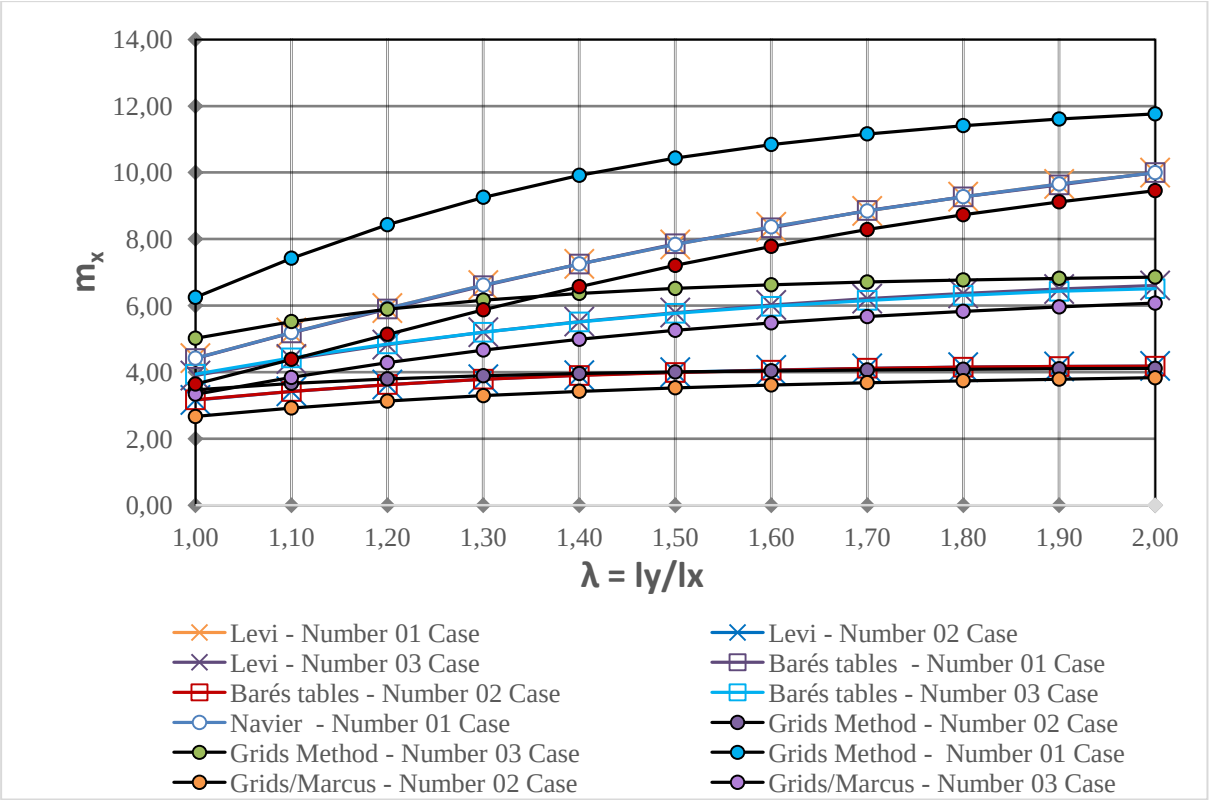

Figure 5. Dimensionless positive bending moments along the "x" direction

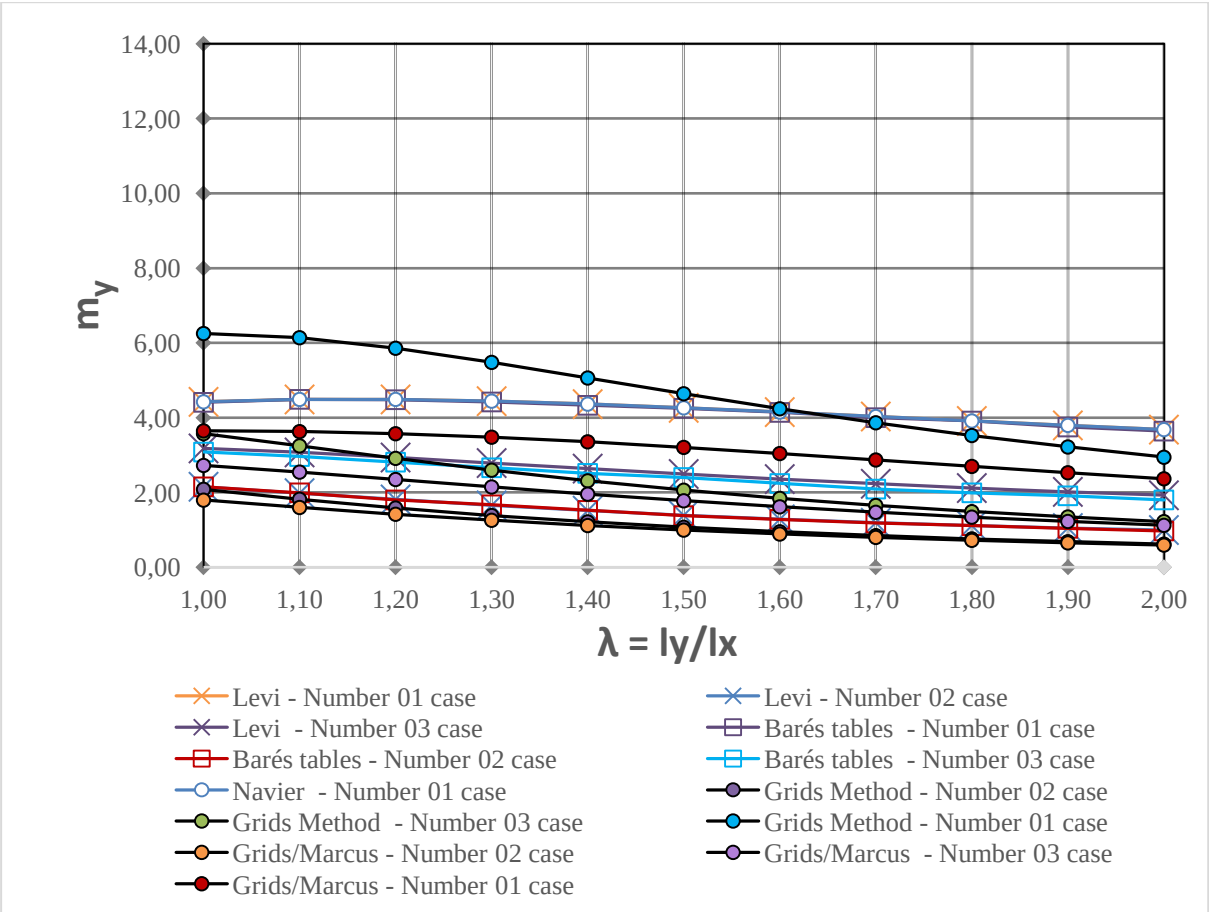

Figure 6. Dimensionless positive bending moments along the "y" direction

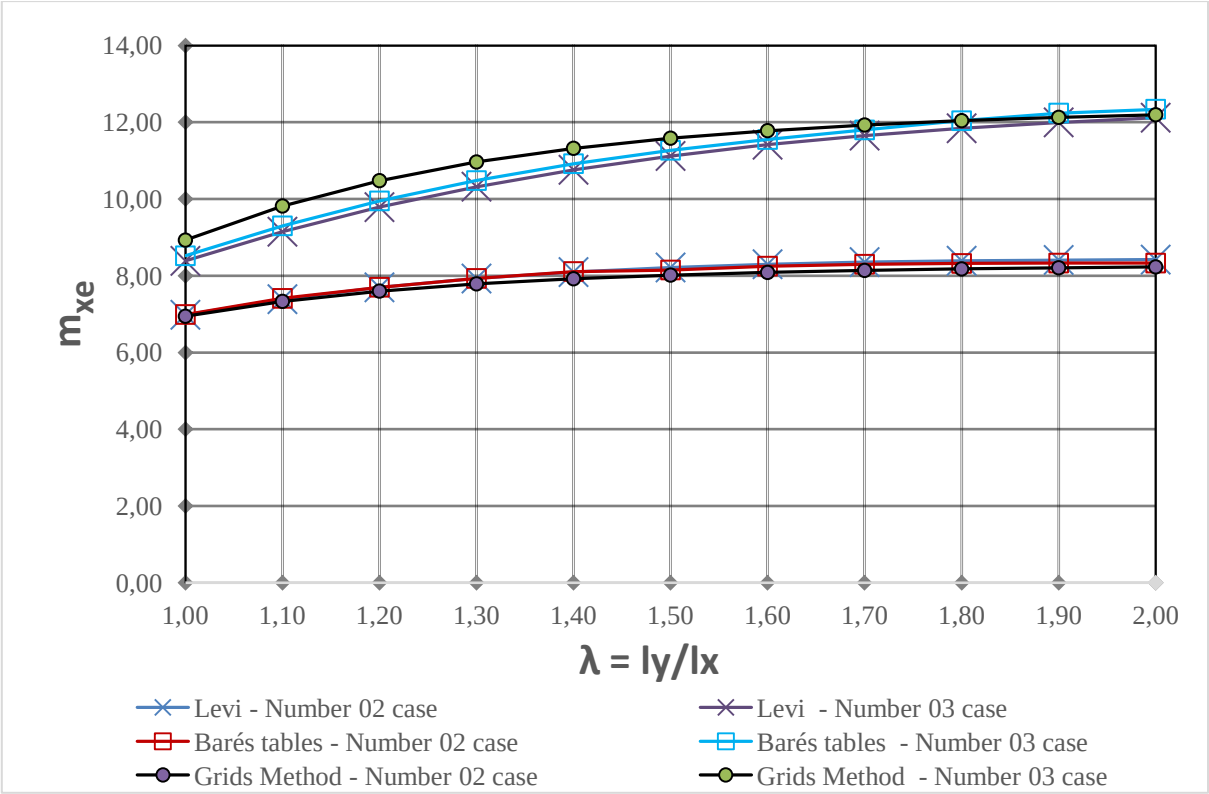

Figure 7. Dimensionless negative bending moments

Table 3. Positive bending moment in "y" coordinate direction dimensionless parameters

	Bending Moment - M_y								
	Number 01 Case			Number 02 Case			Number 03 Case		
λ	P	G	GM	P	G	GM	P	G	GM
1.00	4.42	6.25	3.65	2.15	2.08	1.79	3.18	3.57	2.72
1.10	4.49	6.14	3.63	1.98	1.82	1.60	3.07	3.25	2.54
1.20	4.49	5.86	3.57	1.81	1.58	1.42	2.93	2.91	2.35
1.30	4.44	5.48	3.48	1.66	1.38	1.26	2.79	2.60	2.15
1.40	4.36	5.06	3.35	1.51	1.21	1.11	2.64	2.31	1.95
1.50	4.26	4.64	3.20	1.39	1.07	0.99	2.49	2.06	1.78
1.60	4.15	4.24	3.04	1.28	0.95	0.89	2.36	1.84	1.61
1.70	4.03	3.86	2.87	1.19	0.84	0.80	2.23	1.65	1.47
1.80	3.91	3.52	2.70	1.11	0.76	0.72	2.12	1.49	1.34
1.90	3.79	3.22	2.53	1.05	0.68	0.65	2.02	1.34	1.22
2.00	3.68	2.94	2.36	1.00	0.62	0.59	1.92	1.22	1.12
P – Plates Theory Data; G – Grid Method Data; GM - Grid-Marcus Procedure Data									

The results corresponding to the second stage of analysis, for the slabs whose boundary conditions are illustrated in Fig. 2.a, obtained from the Navier solution, exhibit a good agreement with those ones calculated from the Lévi's trigonometric series, Table 4 and Table 5.

For the case number one, according to the results corresponding to the span length over the "y" coordinate direction "L_y = 6,00 m", specially, once the equilibrium configuration referring to the loading having been reached, the field of the displacements, of the bending moments and of the twisting moments have established themselves as the feature shown in Fig. 8. For the remaining cases such parameters have presented magnitude distribution in a similar way, differentiated, however, among themselves by their numerical values.

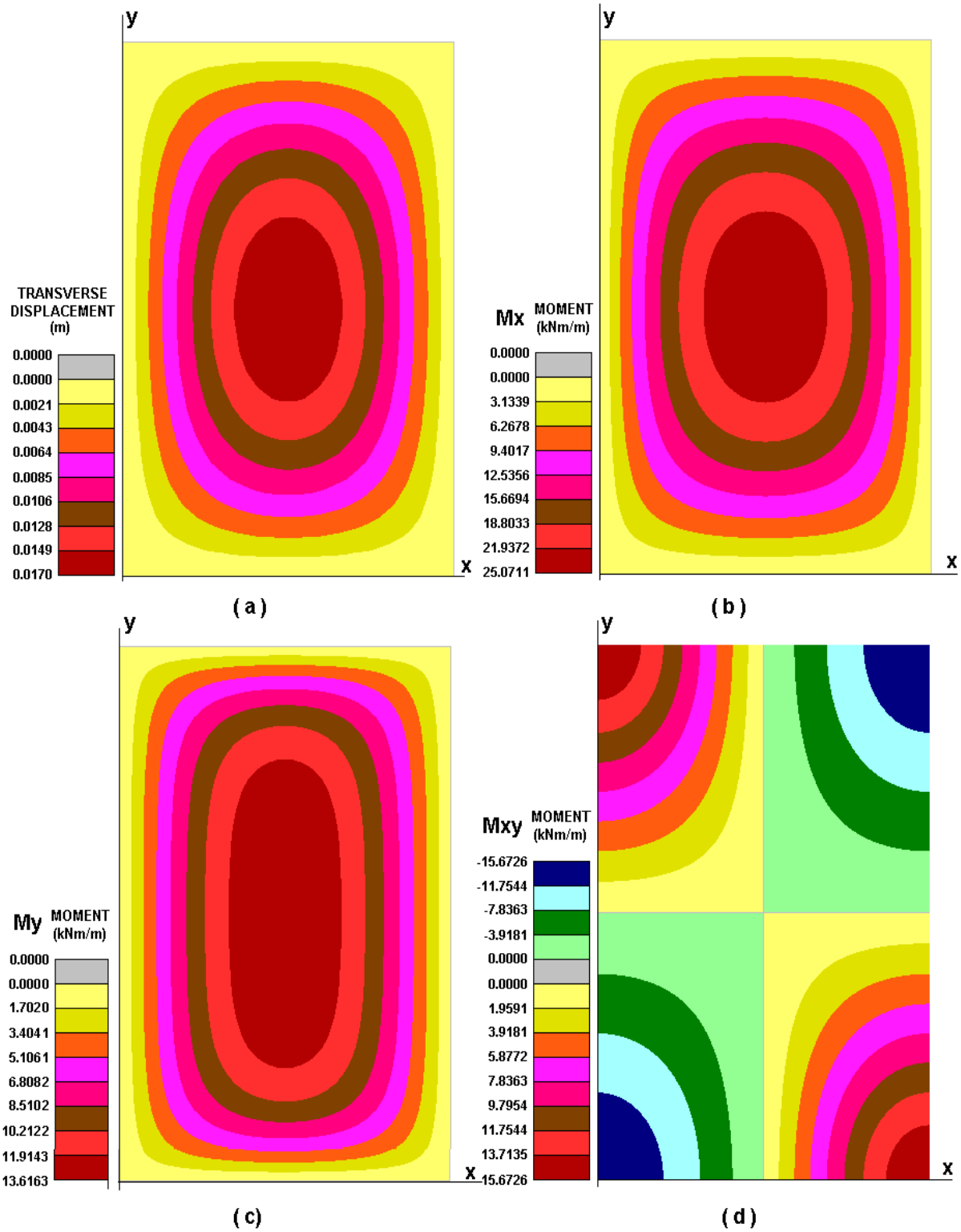

Figure 8. Displacements and Internal Forces Fields – Number one case – 4.00 m x 6.00 m Plate

It may be observed that, in a general way, the fields object of this paper, Fig. 8 and Fig. 9, present shapes according to the traditional knowledge state about the theme approached.

The examination of the field of displacements of the Fig. 9 may induce the wrong idea that on the little width track near the clamped edge of the slab, namely, the track colored by grey chromatic nuance, the transverse displacements would be null. Nevertheless, that fact occurs as a consequence of the adopted precision by the algorithm results that was used in the numerical mapping to the image generation of the referring field.

Table 4. Bending moments at "x" coordinate direction and transverse displacements – number 1 case

x (m)	Transverse Displacements(mm)						Bending Moments M_x (kNm/m)					
	L_y = 4.0 m		L_y = 5.0 m		L_y = 6.0 m		L_y = 4.0 m		L_y = 5.0 m		L_y = 6.0 m	
	$N^{(*)}$	$L^{(**)}$	$N^{(*)}$	$L^{(**)}$	$N^{(*)}$	$L^{(**)}$	$N^{(*)}$	$L^{(**)}$	$N^{(*)}$	$L^{(**)}$	$N^{(*)}$	$L^{(**)}$
0.00	0.0	0.0	0.0	0.0	0.0	0.0	0.0	0.0	0.0	0.0	0.0	0.0
0.50	2.6	2.6	5.0	5.0	6.7	6.7	7.5	7.5	9.8	9.8	11.8	11.8
1.00	4.7	4.7	9.1	9.1	12.2	12.2	11.6	11.6	15.9	15.9	19.4	19.4
1.50	6.0	6.0	11.8	11.8	15.8	15.8	13.6	13.6	19.1	19.1	23.7	23.7
2.00	6.5	6.5	12.7	12.7	17.0	17.0	14.1	14.1	20.1	20.1	25.1	25.1
$N^{(*)}$ – Navier Solution / $L^{(**)}$ – Lévi Solution (kNm/m)												

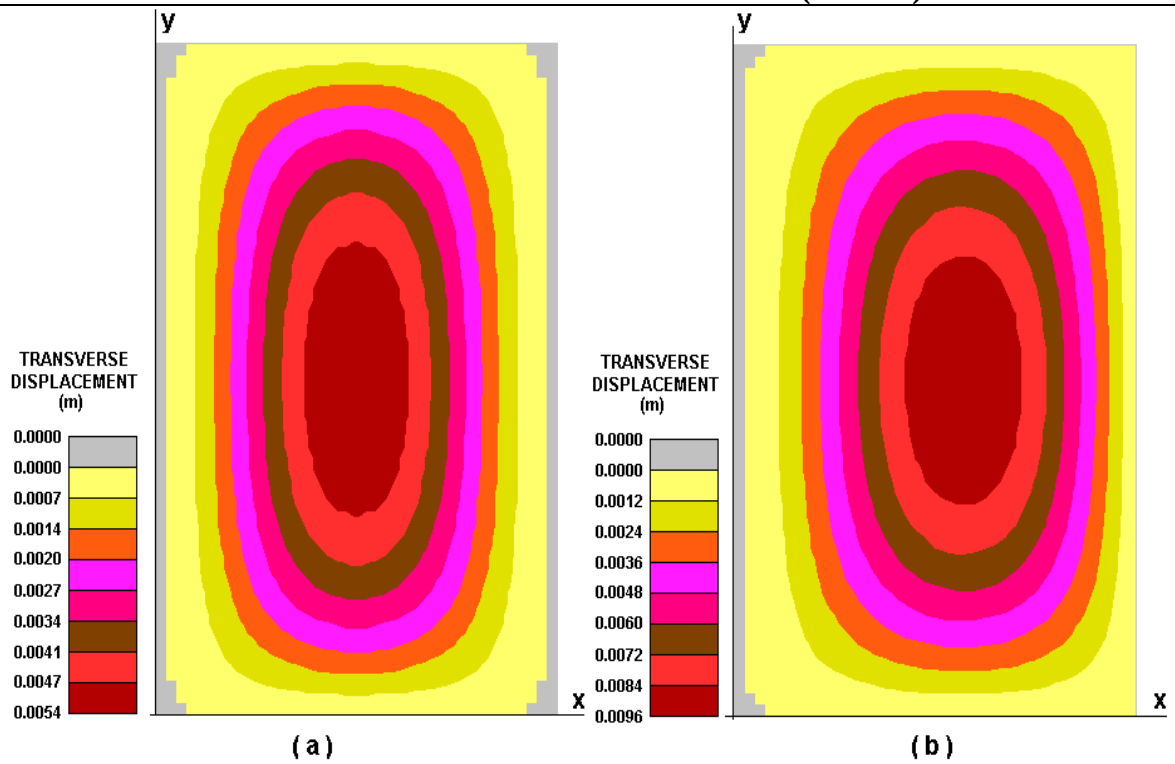

Figure 9. Displacements Fields: a. number 2 case; b. number 3 case

Table 5. Bending Moments at "y" Direction and Twisting Moments – number 1 case

y (m)	Bending Moments M_y (kNm/m)						Twisting Moments M_{xy} (kNm/m)					
	L_y = 4.0 m		L_y = 5.0 m		L_y = 6.0 m		L_y = 4.0 m		L_y = 5.0 m		L_y = 6.0 m	
	$N^{(*)}$	$L^{(**)}$	$N^{(*)}$	$L^{(**)}$	$N^{(*)}$	$L^{(**)}$	$N^{(*)}$	$L^{(**)}$	$N^{(*)}$	$L^{(**)}$	$N^{(*)}$	$L^{(**)}$
0.0	0.0	0.0	0.0	0.0	0.0	0.0	11.9	11.9	14.3	14.3	15.7	15.7
0.5	7.5	7.5	7.3	7.3	7.1	7.1	10.3	10.3	12.8	12.8	14.3	14.3
1.0	11.6	11.6	11.2	11.2	10.8	10.8	7.3	7.3	10.0	10.0	11.6	11.6
1.5	13.6	13.6	13.2	13.2	12.6	12.6	3.8	3.8	6.8	6.8	8.7	8.7
2.0	14.1	14.1	14.1	14.1	13.3	13.3	0.0	0.0	3.4	3.4	5.7	5.7
2.5	***	***	14.3	14.3	13.6	13.6	***	***	0.0	0.0	2.8	2.8
3.0	***	***	***	***	13.6	13.6	***	***	***	***	0.0	0.0
$N^{(*)}$ – Navier Solution / $L^{(**)}$ – Lévi Solution (kNm/m)												

It may be noted that, the Barés tables data, refer themselves to the "M_y" bending moment, correspond to that point of the slab placed at the middle span over the "y" coordinate direction, points C and C' in Fig. 10. However, for the cases involving clamped slabs, if the ratio between the span lengths assumes the highest values, the maximum bending moment over the "y" coordinate direction occurs at points D and D' deviated from that ones, Fig. 10.

Thereby, if "L_y = 6.00 m"**,** the bending moment magnitude for the number 2 case, in the point C vicinity, is "M_y = 1.38 kNm/m"**,** while its maximum value is "M_y = 1.78 kNm/m", corresponding to a difference by approximately 29%**.** For the number 3 case, in the other hand, the bending moment magnitude close to the point C', is "M_y = 2.40 kNm/m" while "M_y = 2.61 kNm/m" is its maximum value, corresponding to a difference by the order of 9%**.**

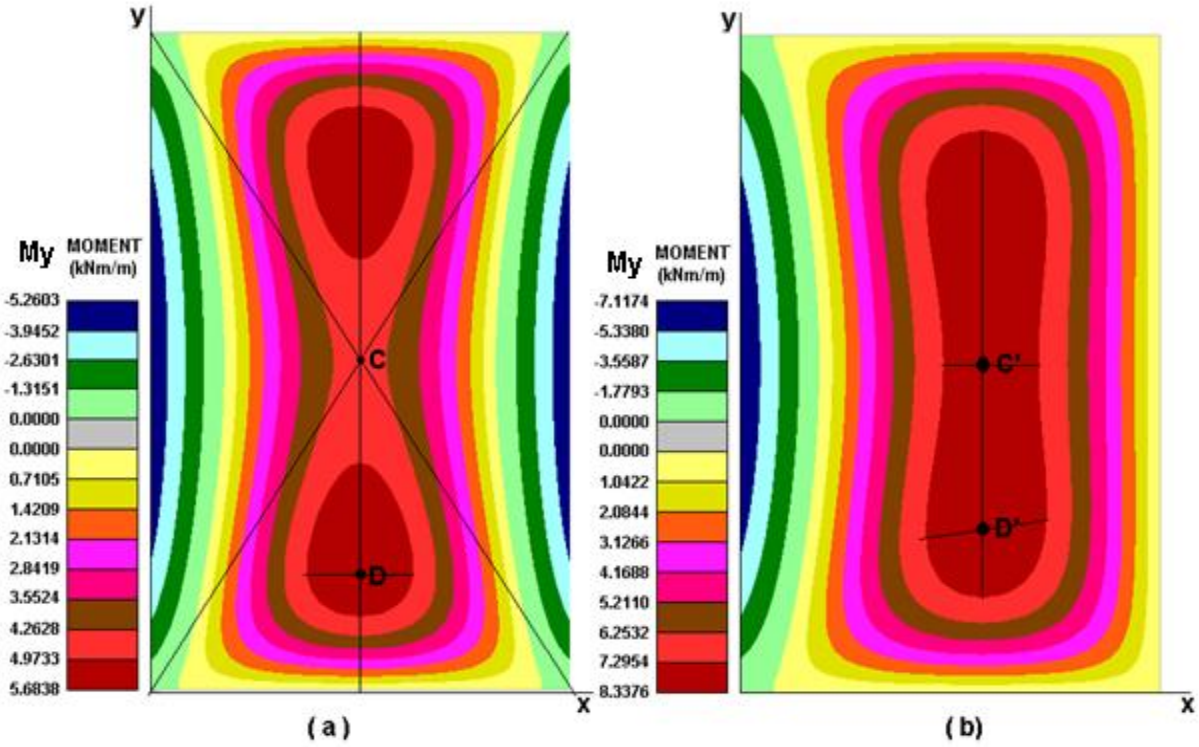

Figure 10. M_y Bending Moment Fields: a. number 2 case; b. number 3 case

7 Conclusions

The mechanical performance comparative analysis of slabs from the Kirchhoff's Theory, from the Grids Method, from the Marcus Method and from the Barés Table is carried out in this paper.

The analysis was performed upon three different types of slabs according its boundary conditions, namely, simple supported along its all four edge, clamped along one edge and simple supported in the remain ones, and, clamped along two opposite edges and simple supported along the others ones.

At first, it was considered 11 (eleven) different values for the ratio involving the span lengths along the two coordinate directions, namely, 1.0; 1.1; 1.2; 1.3; 1.4; 1.5; 1.6; 1.7; 1.8; 1.9 and 2.0, and then the dimensionless parameters referring to displacements and internal forces were calculated.

On a second stage of this work, for the same boundary condition already characterized above in these conclusions, the analysis from the consideration of three different span lengths in the "y" direction, namely: "L_y = 4.00 m"; "L_y = 5.00 m"; and, "L_y = 6.00 m" was performed.

At the first stage of the analysis, it was found from the obtained results a close agreement between the Barés tables data and those results determined from the Kirchhoff's Theory.

The referring results also revealed that the displacement magnitudes and the positive bending moments calculated from the Grids Method have presented values greater than those one determined from the Kirchhoff's Theory, because, the Grids Method neglects the shear stiffness.

The differences between the displacement magnitudes reported above are as smaller as greater the ratio between the span lengths along the two coordinate directions, and are too considerable if one paying attention to the reality that the displacement magnitudes by time, according to the Brazilian technical standard NBR 6118/2014 recommendation, are, already overrated.

In addition, it was observed that, the positive bending moments determined from the Grid-Marcus Method have presented the smallest values among those results obtained from all models that are being considered in this paper.

The differences referring in the last two paragraphs were as smaller as greater was the ratio between the span lengths and were as greater as smaller the slab flexure stiffness.

Due to the bending moment magnitude reduction in the "x" direction promoted by the plastic fitting process, the difference in their magnitude must be decreased, and then, the Marcus's Method may be considered suitable for their values determination.

On the other hand, the bending moment magnitude increase in the "y" direction, caused by the same process referred in the last paragraph, makes the difference mentioned above in this text higher, revealing, consequently, the needing for the Marcus's adjuster coefficients evaluation improvement.

The acquired results reveal a satisfactory agreement among all the adopted data sources on regard to the negative bending moments.

From the fields images, whose generation were the subject of the second stage of the analysis carried out in this paper, it may be observed a good agreement between the Navier's solution and the results obtained by the Lévi's series.

In addition, it may be observed that, the Barés table present the value of the bending moment in the "y" direction for a point placed on the center of the slab while for the number 02 and number 03 cases, the maximum values of such internal force, according to Lévi's solution, occurs at a deviate region apart from that point.

The resulting difference between the bending moment magnitude in the "y" direction obtained by Barés table and its corresponding maximum values calculated from Lévi's solution, may reach up to 29%, so that, if the design engineer uses the Barés tables data to perform design of slabs, such a procedure may promote the material failure risk.

Acknowledgements

This report is part of a research work on the numerical simulation of the mechanical performance of slabs supported by the Pró-Reitoria de Pesquisa of the Universidade Federal do Rio Grande do Norte – UFRN. This support is gratefully acknowledged.

References

[1] S. Timoshenko and S. Woinowsky-Krieger. Theory of Plates and Shells. *2ª Edição. McGraw-Hill, Londres, 1989.*

[2] R. Szilard. Theories and Applications of Plate Analysis. John Willey & Sons, Inc., 2004.

[3] J. M. Araújo. Curso de Concreto Armado. Volume 2. Editora Dunas. Rio Grande, 2014.

[4] R. D. Cook, D. S. Malkus, and M. E. Plesha. Concepts and Applications of Finite Element Analysis. John Wiley e Sons. Nova York, 1989.

[5] E. L. Madureira and A. L. A. Silva. Project1 – Programa para visualização de campos de tensões resultantes de analises não lineares de modelos bidimensionais de elementos finitos. Versão 1.0, Rio Grande do Norte: DEC/UFRN, 2013.

[6] Associação Brasileira de Normas Técnicas. NBR 6118/2014**.** Projeto de Estruturas de Concreto Armado - Procedimento, 2014.

[7] A. L. A. Silva and K. Cashell. Ultimate Behaviour in Composite Floor Slabs. Summer Project for Study Abroad Programmes. Londres. Brunel University, 2015.

[8] E. L. Madureira, E. M. Medeiros and A. L. A. Silva. Análise Numérica Comparativa de Modelos Aplicáveis ao Projeto de Lajes de Concreto. 59 Congresso Brasileiro do Concreto. Bento Gonçalves, 2017.